I. Troch, F. Breitenecker, eds. ISBN 978-3-901608-35-3

# MULTIPORT COMMUNICATION MODEL OF THE LOW-VOLTAGE POWER LINE NETWORK

Nermin Suljanović [1], Aljo Mujčić [1], Amer Hasanović [1], Matej Zajc [2], Jurij Tasič [2]
[1]Faculty of Electrical Engineering University of Tuzla, Bosnia and Herzegovina; [2]Faculty of Electrical Engineering University of Ljubljana, Slovenia

Corresponding Author: Nermin Suljanović, Faculty of Electrical Engineering Tuzla, University of Tuzla , 75000 Tuzla, Franjevačka 2, Bosnia and Herzegovina, Email: nermin.suljanovic@untz.ba

**Abstract**. This paper presents a methodology for modeling the communication characteristics for low-voltage (LV) power lines. The derived model can be utilized for the design of digital communication systems via LV power networks. Simulation results are demonstrated for a 50 m long power cable.

## 1 Introduction

Power lines are primarily used for the transmission of electric power. During the last fifty years different models of utilization of power lines for the transfer of information have been implemented. However, during the analogue era, communications via power lines, also known as power-line carrier (PLC), was mainly used by power utilities for their internal purposes. Development and deployment of digital communication techniques gave possibility to extend PLC services to domains such as Internet, VoIP, SCADA etc.

Taking into consideration the differences in communications channel, the PLC systems are classified into two categories. High Voltage (HV) PLC systems, which allow data transfers at longer distances (hundreds of kilometers) with rather low data rates (64 kbps), and Low Voltage (LV) PLC systems, which are useful for shorter distances (hundreds of meters) with significantly higher bit rates (in range of Mbps).

Proper design of digital communication systems requires the specification of the following communications channel characteristics: amplitude characteristics, group delay and input impedance. PLC communication utilizes a frequency spectrum in the MHz range regardless of the underlying power network. Since the power grids are optimized for the transfer of electric power and not for the flow of information, there is an increased need for modelling of PLC, especially for LV PLC, in order to adequately estimate the degradation introduced in the communications channel.

This paper presents a modelling methodology of LV PLC channel based on a multiport analysis and telegraphers' equations in the matrix form. Representing power-line cables in the form of multiconductor system, LV PLC channel communication characteristics are determined in the radio-frequency range and are derived for different coupling schemes of communication equipment with the respect to the power line. Deterministic approach presented in the paper is focused on the point-to-point communication via power line, but is appropriate to be extended to the branched structure of the low-voltage power grid.

## 2 Signal propagation via multiconductor low-voltage power lines

Low-voltage power lines are multiconductor lines and their modeling is based on equations of telegraphy in the matrix form. These equations are reduced for the sinus wave propagation and solution is derived for the frequencies of the interest in order to obtain amplitude characteristic and group delay. Since inductive and capacitive coupling between conductors exists, equations are coupled. Modal analysis, based on the eigenvalue and eigenvectors decomposition, is utilized for decoupling of the equations.

### 2.1 Telegraphers' equations

The wave propagation phenomena along the power line are described by equations of telegraphy. Since the power line is considered as a multiconductor line, voltage **V** and current **I** at the arbitrary point on power line are found from the equations of telegraphy in the matrix form [1]:

$$\frac{d^2\mathbf{V}}{dx^2}-\mathbf{ZYV}=\frac{-d\,\mathbf{E}(x)}{dx}+\mathbf{ZJ}(x) \tag{1}$$

$$\frac{d^2\mathbf{I}}{dx^2}-\mathbf{YZV}=\frac{-d\,\mathbf{J}(x)}{dx}+\mathbf{YE}(x) \tag{2}$$

Elements of matrices **Z** and **Y** form the set of primary parameters of the power line parallel to the earth plane. Those parameters are determined by geometrical design of the power line and electrical parameters of the conductors and earth [2]. Any primary parameter is frequency dependent. Matrices **E(x)** and **I(x)** represent voltage and current sources distributed along the line. In the case of the passive network their values are equal to zero.

### 2.2 Equations of telegraphy solution: Modal analysis

Equations (1) and (2) are written in original (phase) coordinates. The solution of these equations is found through the modal transformation [1, 3-5]:

$$\mathbf{V}=\mathbf{S}\cdot\mathbf{V}_s,\ \mathbf{I}=\mathbf{Q}\cdot\mathbf{I}_s \tag{3}$$

which introduces modal coordinates where voltage and current are described with vectors $\mathbf{V}_s$ and $\mathbf{I}_s$.

Complex matrix **S** is chosen to be a matrix of eigenvectors of product $\mathbf{\Gamma}^2=\mathbf{ZY}$ while $Q=(S^T)^{-1}$. $\mathbf{\Gamma}$ denotes propagation function matrix in original coordinates. Applying transformation defined with expression (3), equations (1) and (2) become a set of ordinary nonhomogeneous differential equations that can be written in the matrix form:

$$\frac{d^2\mathbf{V}_s}{dx^2}=\boldsymbol{\gamma}^2\mathbf{V}_s+\mathbf{Z}_s\mathbf{J}_s(x)-\frac{d\,\mathbf{E}_s(x)}{dx} \tag{4}$$

$$\frac{d^2\mathbf{I}_s}{dx^2}=\boldsymbol{\gamma}^2\mathbf{I}_s+\mathbf{Y}_s\mathbf{E}_s(x)-\frac{d\,\mathbf{J}_s(x)}{dx} \tag{5}$$

# 3 High-frequency characteristics of the LV power line

There are two major deterministic approaches to LV power-line transfer function modelling, in the sense of point-to-point communication. First, power-line multiport representation and reduction of ports in respect to used coupling and second, computation of voltages and currents at second power-line end incorporating reflection coefficients [1, 3-5]. In the paper power-line model derived through the second approach is presented. The first approach gives equal results for homogeneous power lines as the second one, but some difficulties can arise with nonhomogeneous power lines represented with multiport cascades (for instance, existence of branches or shunt impedances).

When $\bar{V}_1$ and $\bar{I}_1$ are known sinusoidal voltage and current of arbitrary frequency *f* at the transmitting end and $\bar{V}_2$ and $\bar{I}_2$ are computed voltage and current at receiving end, power-line transfer function is defined with the amplitude characteristic:

$$\alpha=10\log\frac{|\bar{V}_2\bar{I}_2|}{|\bar{V}_1\bar{I}_1|}\quad[dB] \tag{6}$$

and phase characteristic:

$$\beta=\Im\frac{|\bar{V}_2|}{|\bar{V}_1|}\quad[rad] \tag{7}$$

Nonlinearities in the phase characteristics are well observed if instead of phase is used a phase derivative versus frequency, known as a group delay. The group delay is defined as

$$\tau=-\frac{d\beta}{d\omega}=-\frac{1}{2\pi}\frac{d\beta}{df} \tag{8}$$

Voltages and currents in equations (6) - (8) depend on the scheme how transmitter and receiver are connected to the power line, what we in practice call coupling. Different couplings excite different modes and therefore, are characterized with different transfer functions. The couplings used in the practice correspond to the transmitter and receiver connection between one phase and ground or between two phases.
In order to define algorithm for computation of homogeneous LV power line transfer function, transmitter and receiver models are given. This is fundamental for the voltage and current computations at both line terminals.

# 4 Transmitter and receiver model

The transmitter is usually modeled in one of two modeling ways [3, 4]:

1.As a time-harmonic voltage generator in serial with an impedance;

2.As a time-harmonic current generator in parallel with an admittance.

Voltage generators and impedances can be connected between any two conductors (or ports of the multiport that replaces the power line) or a conductor and the ground. This is schematically presented in Figure 1. Analogue worth for the model with the current generators.

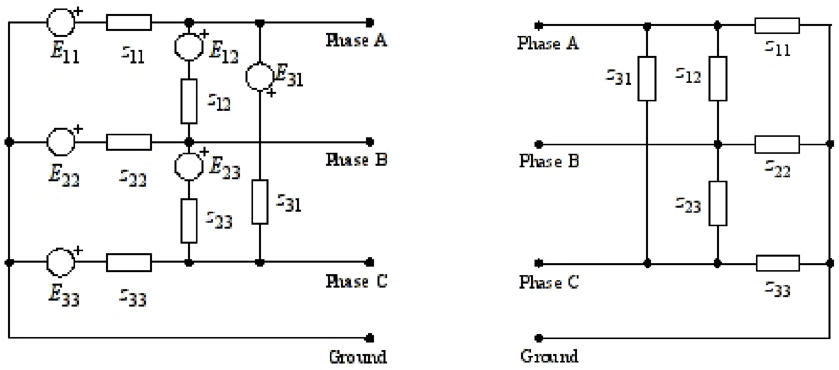


a) Transmitter model  b) Receiver model

**Figure 1.** Transmitter and receiver model

Lets denote the sinusoidal voltages at arbitrary frequency of phase A, B and C to the ground with the column vector $\mathbf{V}_1$. Currents flowing into the power line are denoted with the column vector $\mathbf{I}_1$. We will assume that voltage generators are connected between a phase conductor and the ground. In such manner, voltage sources are represented with a vector column $\mathbf{E}_g$. If $\mathbf{Y}_{in}$ represents the input admittance at the transmitting power-line terminal, the voltage and current at the transmitting terminal are [3, 4]:

$$\mathbf{I_1 = Y_g (I + Y_g Z_{in})^{-1} E_g} \tag{9}$$

$$\mathbf{V_1 = Y_g (Y_g + Y_{in})^{-1} E_g} \tag{10}$$

where $\mathbf{Y}_g$ is the admittance matrix defined by:

$$\mathbf{Y_g} = \begin{bmatrix} \sum_{k=1}^{N} y_{1k} & -y_{12} & \cdots & -y_{1N} \\ -y_{12} & \sum_{k=1}^{N} y_{2k} & \cdots & -y_{2N} \\ . & . & \cdots & . \\ -y_{1N} & -y_{2N} & \cdots & \sum_{k=1}^{N} y_{Nk} \end{bmatrix} \tag{11}$$

The transmitter model with the current generator is defined with vector $\mathbf{I}_g$ found from:

$$\mathbf{I_g = Y_g E_g} \tag{12}$$

The voltage and current at the transmitting terminal equals

$$\mathbf{V_1 = (Y_g + Y_{in})^{-1} I_g} \tag{13}$$

$$\mathbf{I_1 = Y_{in} (Y_g + Y_{in})^{-1} I_g} \tag{14}$$

The receiver is modeled with a passive network (Figure 1) and represented in the matrical form with load admittance $\mathbf{Y}_L$.

## 5 Determination of the voltage at the receiving power line terminals

Frequency characteristics can be determined from the equations (6) - (8) if voltages and currents at the receiving power-line terminals are computed for known voltages and currents at the transmitting power-line terminal. This sections presents an algorithm for received voltages and currents computation utilizing modal theory. Algorithm is matrix oriented and therefore appropriate for the computer simulations.

The voltage and current at the transmitting line terminal are interrelated through the input admittance (or input impedance) matrix

$$\mathbf{I_1 = Y_{in} V_1 = Z_{in}^{-1} V_1} \tag{15}$$

and at the receiving end with the load admittance matrix

$$\mathbf{I_2 = Y_L V_2 = Z_L^{-1} V_2} \tag{16}$$

The voltage and current at the line terminal is a sum of incident and reflected signal components:

$$\mathbf{V_2} = \mathbf{V_2^+} + \mathbf{V_2^-} \tag{17}$$

$$\mathbf{I_2} = \mathbf{I_2^+} + \mathbf{I_2^-} = \mathbf{Y_c}(\mathbf{V_2^+} - \mathbf{V_2^-}) \tag{18}$$

Solving the set of previous equations we obtain

$$\mathbf{V_2^+} = \frac{1}{2}(\mathbf{I} + \mathbf{Z_c}\mathbf{Y_L})\mathbf{V_2}, \mathbf{V_2^-} = \frac{1}{2}(\mathbf{I} - \mathbf{Z_c}\mathbf{Y_L})\mathbf{V_2} \tag{19}$$

A reflection coefficient represents a ratio between reflected and incident waves. In the case of multiconductor system, the reflection coefficient is a square matrix interrelating reflected and incident waves at different ports:

$$\mathbf{V_1^-} = \mathbf{K_1}\mathbf{V_1^+}, \quad \mathbf{V_2^-} = \mathbf{K_2}\mathbf{V_2^+} \tag{20}$$

Utilizing equations (17)-(20), matrical reflection coefficient at the receiving terminal is obtained:

$$\mathbf{K_2} = (\mathbf{I} + \mathbf{Z_c}\mathbf{Y_L})^{-1}(\mathbf{I} - \mathbf{Z_c}\mathbf{Y_L}) \tag{21}$$

Analogously, the voltage at the sending line terminal can be expressed in the term of the incident wave and matrical reflection coefficient [1]:

$$\mathbf{V_1} = \mathbf{V_1^+} + \mathbf{V_1^-} = (\mathbf{I} + \mathbf{K_1})\mathbf{V_1^+} \tag{22}$$

Since the incident voltage at the receiving line end is determined by the propagation function and the power-line length

$$\mathbf{V_2^+} = \mathbf{exp}(-\boldsymbol{\Gamma}\,\mathbf{l})\mathbf{V_1^+} \tag{23}$$

the voltages at the receiving and sending line ends are interrelated with equation

$$\mathbf{V_2} = (\mathbf{I} + \mathbf{K_2})\mathbf{exp}(-\boldsymbol{\Gamma}\,\mathbf{l})(\mathbf{I} + \mathbf{K_1})^{-1}\mathbf{V_1} = \mathbf{T}\mathbf{V_1} \tag{24}$$

where matrix T is the voltage transfer matrix.

The matrical reflection coefficient is yielded by interrelating reflected and incident waves at the sending line terminal [1, 3-5]:

$$\mathbf{K_1} = \mathbf{exp}(-\boldsymbol{\Gamma}\,\mathbf{l})\mathbf{K_2}\mathbf{exp}(-\boldsymbol{\Gamma}\,\mathbf{l}) \tag{25}$$

while the input admittance is:

$$\mathbf{Y_{in}} = \mathbf{Y_c}(\mathbf{I} - \mathbf{K_1})^{-1}(\mathbf{I} + \mathbf{K_1})^{-1} \tag{26}$$

## 6 The transfer function computation for the multiconductor power line

The equations determining transfer function (amplitude and phase characteristic and group delay) and input line impedance are derived in this section for the case of three-conductor line (Figure 2). The same approach may be extended to a case with arbitrary number of the conductors.

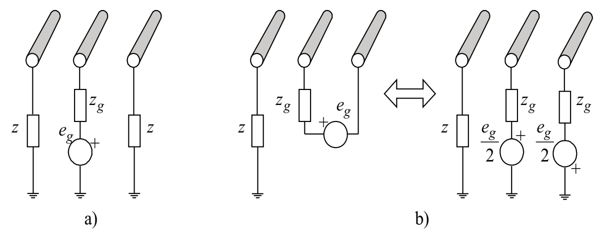


**Figure 2.** A principal scheme of a phase to ground coupling (a) and a phase to phase coupling (b)

Voltages at the sending and the receiving end of a multiconductor transmission line are related with the voltage transfer matrix **T**. Corresponding currents are determined with the termination admittances at the both power-line ends, denoted with matrices $\mathbf{Y}_g$ and $\mathbf{Y}_L$. The transfer function of a multiconductor transmission line are computed directly from the voltage transfer matrix, utilizing information of relations between the voltages at the both line ends contained in the matrix **T**.

A problem that arises in such formulae derivations is related to a multiconductor system where the voltages of all output ports are related to the all voltages of all input ports. In the further analysis we will find a solution to this problem by expressing all port voltages in the terms of one port voltage. Due to simplicity we are beginning with the analysis of a conductor (phase) to ground coupling. We will suppose that the transmitter is modeled as the voltage generator, represented by the voltage column vector $\mathbf{E}_g$ and the impedance matrix $\mathbf{Z}_g$. When the voltage source impedance is $z_g$, we can set a relation that defines voltages of all three phases at the sending line terminal as:

$$\mathbf{V_1}=\mathbf{Y}_\Sigma^{-1}=\frac{1}{z_g}(\mathbf{Y_g}+\mathbf{Y_{in}})^{-1}\mathbf{E_g}=\mathbf{L}\,\mathbf{E_g} \tag{27}$$

$$\mathbf{I_1}=\mathbf{Y_{in}}\mathbf{V_1} \tag{28}$$

The nodal current matrix is determined in accordance with the method of the node voltages while the matrix **L** is a square matrix whose dimensions are determined by the number of conductors.

At the beginning lets consider conductor $k$ to ground coupling at the sending and phase $t$ to ground at the receiving end. Amplitude and phase characteristic are computed as:

$$\alpha=10\log\left|\frac{V_2(t)I_2(t)}{V_1(t)I_1(t)}\right| \tag{29}$$

$$\beta=\Im\left\{\ln\frac{V_2(t)I_2(t)}{V_1(t)I_1(t)}\right\} \tag{30}$$

while the input impedance is

$$Z_{\mathrm{in}}=\frac{V_1(k)}{I_1(k)} \tag{31}$$

The k-th element in the vector $\mathbf{E}_\mathrm{g}$ equals $e_g$, while other elements are zero. Applying this in equation (29), voltage at the sending end is found to be:

$$\mathbf{V_1}=\mathbf{L_k}\,e_g \tag{32}$$

where $\mathbf{L}_k$ is $k$-th column of the matrix **L**. As we mentioned at the beginning of the section, we need to express all phase voltages in the term of one parameter. For instance, voltage of the first port at the sending end can be chosen as such parameter. The ratio between the voltage of the conductor $i$ and the voltage of conductor 1 is

$$\frac{V_1(i)}{V_1(1)}=\frac{L(i,k)}{L(1,k)},\quad i=1,2,\ldots n \tag{33}$$

At this point we introduce the vector $\mathbf{L}_\mathrm{kr}$ whose element $i$ is defined by equation (33). Now, vector $\mathbf{V}_1$ is expressed in the term of $V_1(1)$:

$$\mathbf{V_1}=\mathbf{L_{kR}}V_1(1) \tag{34}$$

Further we rewrite the voltage at the receiving end in the term of parameter $V_1(1)$:

$$\mathbf{V_2}=\mathbf{TL_{kR}}V_1(1) \tag{35}$$

The voltage of the conductor t at the receiving end is found to be equal

$$V_2(t)=\mathbf{TL_{kR}}V_1(1) \tag{36}$$

where is a row $t$ of the matrix **T**. At this point we miss only an expression for the currents at the both line ends.

It is obvious that the current at the sending end equals

$$\mathbf{I_1}=\mathbf{Y_{in}}\mathbf{L_{kR}}V_1(1) \tag{37}$$

while the current at the receiving end is

$$\mathbf{I_2}=\mathbf{Y_L}\,\mathbf{T}\,\mathbf{L_{kR}}V_1(1)=\mathbf{F}\,\mathbf{L_{kR}}V_1(1) \tag{38}$$

where **F** is the auxiliary square matrix. If with $\mathbf{Y}^\mathrm{k}_\mathrm{in}$ we denote *k-th* row in the input admittance matrix $\mathbf{Y}_\mathrm{in}$ and with $\mathbf{F}_\mathrm{t}$ row $t$ in the matrix **F**, then the voltage of phase $k$ at the sending end and the voltage of the phase $t$ at the receiving end are respectively

$$I_1(k)=\mathbf{Y_{in}^k}\mathbf{L_{kR}}V_1(1) \tag{39}$$

$$I_2(t)=\mathbf{B_t}\mathbf{L_R}V_1(1) \tag{40}$$

Substituting the expressions for the both line ends in the equations from (29) to (31) we found

$$\alpha = 10\log\left|\frac{\mathbf{T_t}\mathbf{L_R}}{\mathbf{L_{kR}}(k)}\frac{\mathbf{Y_{in}^k}\mathbf{L_{kR}}}{\mathbf{B_t}\mathbf{L_{kR}}}\right| \quad [dB] \tag{41}$$

$$\beta = \Im\left\{\ln\frac{\mathbf{T_t}\mathbf{L_R}}{\mathbf{L_{kR}}(k)}\frac{\mathbf{Y_{in}^k}\mathbf{L_{kR}}}{\mathbf{B_t}\mathbf{L_{kR}}}\right\} \quad [rad] \tag{42}$$

$$Z_{\text{in}} = \frac{\mathbf{L_{kR}}(k)}{\mathbf{Y_{in}^k}\mathbf{L_{kR}}} \tag{43}$$

The three preceding equations define transfer function of the transmission line with three conductors when the transmitter and the receiver are connected between one conductor and the ground (phase to ground coupling in the case of power line). Similar analysis can be conducted for the case where communication equipment is connected between two arbitrary conductors of a transmission line (phase to phase coupling in the case of power line). Lets assume the coupling conductor $j$ to conductor $k$ at the sending line terminal and conductor $s$ to conductor $t$ at the receiving terminal. The elements of the voltage vector $\mathbf{E}_g$ are equal to zero, except $s$-th and $k$-th elements which are

$$E_g(j) = e_g/2, \quad E_g(k) = -e_g/2 \tag{44}$$

If $\mathbf{L}_j$ and $\mathbf{L}_k$ denote $j$-th and $k$-th columns of the matrix $\mathbf{L}$ respectively, the voltage at the sending terminal is

$$\mathbf{V_1} = (\mathbf{L_j} - \mathbf{L_k})\frac{e_g}{2} = \mathbf{L_{jk}}\frac{e_g}{2} \tag{45}$$

Likewise the phase to ground coupling, elements of voltage vector $\mathbf{V}_1$ are expressed in the term of voltage $V_1(1)$ utilizing vector column $\mathbf{L}_{jkR}$ whose elements are

$$\mathbf{L_{jkR}} = \frac{V_1(i)}{V_1(1)} = \frac{L_{jk}(i)}{L_{jk}(1)} = \frac{L(i,j) - L(i,k)}{L(1,j) - L(1,k)}, \quad i = 1, \ldots n \tag{46}$$

The voltage at the sending end is then

$$\mathbf{V_1} = \mathbf{L_{jkR}} V_1(1) \tag{47}$$

and for the selected coupling

$$V_1(j) - V_1(k) = \left(L_{jkR}(j) - L_{jkR}(k)\right) V_1(1) \tag{48}$$

Voltage at the receiving end is related to the voltage at the sending end with the voltage transfer matrix

$$\mathbf{V_2} = \mathbf{T}\,\mathbf{L_{jkR}} V_1(1) \tag{49}$$

while the voltage at the receiver is

$$V_2(s) - V_2(t) = (\mathbf{T_s} - \mathbf{T_t})\mathbf{L_{jkR}} V_1(1) \tag{50}$$

The currents at the power line terminals are

$$\mathbf{I_1} = \mathbf{Y_{in}}\mathbf{L_{jkR}} V_1(1) \tag{51}$$

$$\mathbf{I_2} = \mathbf{Y_L}\,\mathbf{T}\,\mathbf{L_{jkR}} V_1(1) = \mathbf{F}\,\mathbf{L_{jkR}} V_1(1) \tag{52}$$

Since $\mathbf{Y}_{\text{in}}^{j}$ represents the $j$-th row of matrix $\mathbf{Y}_{\text{in}}$ and $\mathbf{F}_s$ corresponds to the $s$-th row of the matrix $\mathbf{B}$, currents at the receiver and at the transmitter respectively are:

$$I_1(j) = \mathbf{Y}_{\text{in}}^{j}\mathbf{L_{jkR}} V_1(1) \tag{53}$$

$$I_2(s) = \mathbf{B_s}\mathbf{L_{jkR}} V_1(1) \tag{54}$$

The high-frequency power-line channel characteristics are then derived from equations (48), (50), (53) and (54) :

$$\alpha = 10\log\left|\frac{V_2(s) - V_2(t)}{V_1(j) - V_1(k)}\cdot\frac{I_2(s)}{I_1(j)}\right| = 10\log\left|\frac{(\mathbf{T_s} - \mathbf{T_t})\mathbf{L_{jkR}}}{L_{jkR}(j) - L_{jkR}(k)}\cdot\frac{\mathbf{B_s}\mathbf{L_{jkR}}}{\mathbf{Y}_{\text{in}}^{j}\mathbf{L_{jkR}}}\right| \quad [dB] \tag{55}$$

$$\beta = \Im\left\{\ln\left\{\frac{V_2(s) - V_2(t)}{V_1(j) - V_1(k)}\right\}\right\} = \Im\left\{\ln\left\{\frac{(\mathbf{T_s} - T_t)\mathbf{L_{jkR}}}{L_{jkR}(j) - L_{jkR}(k)}\right\}\right\} \quad [rad] \tag{56}$$

$$Z_{\text{in}} = \frac{V_1(j) - V_1(k)}{I_1(j)} = \frac{L_{jkR}(j) - L_{jkR}(k)}{\mathbf{Y}_{\text{in}}^j \mathbf{L}_{\mathbf{jkR}}} \quad (57)$$

## 7 Simulation results for 220 V power line

In this section we present and discuss simulation results for the point to point communication via LV power line. Multipath propagation is not considered, but approach presented in the paper can be extended to the branched structure of the LV power grid. This is achieved by introducing shunt impedances that correspond to the input impedance of the branch power line. Since input impedances are frequency-dependant, reflection at the branch line terminals are included in the model.

Signal propagation via LV multiconductor power line is described by telegrapher's equations (1) and (2). Corresponding imppedance **Z** and admitance matrices **Y** are:

$$\mathbf{Z} = \mathbf{R} + j\omega\mathbf{L}, \quad \mathbf{Y} = \mathbf{G} + j\omega\mathbf{C} \quad (58)$$

For the power distribution cables, with the cross-section represented in Figure 3, matrices **L** and **C** are symmetric and take the form [Grassi]:

$$\mathbf{L} = \begin{bmatrix} l_a & l_a - l_b & l_b \\ l_a - l_b & l_a & l_b \\ l_b & l_b & 2l_b \end{bmatrix}, \quad \mathbf{C} = \begin{bmatrix} c_a & 2c_b - c_a & -c_b \\ 2c_b - c_a & c_a & -c_b \\ -c_b & -c_b & c_a \end{bmatrix} \quad (59)$$

We will make an assumption that the conductance **G** equals zero matrix, while the resistance **R** is determined at the PLC frequencies by the skin effect. In the MHz range, devoted to LV PLC systems, resistance due to the skin effect is [Berrysmith]:

$$R = \sqrt{\frac{\pi \mu_0 f}{\kappa r^2}} \quad (60)$$

where $r$ is radius of the corresponding phase conductor and $\kappa$ is conductivity of the conductor. Values R are further elements of the diagonal matrix **R**. All presented matrices **R**, **L** and **C** are considered to be 3x3 matrices since the fourth null conductor is usually grounded and therefore is not utilized for the signal propagation. Influence of the fourth conductor to the signal propagation is incorporated in the matrices **L** and **C**.

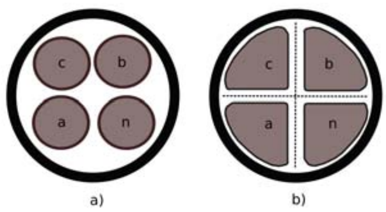


Figure 3. Cross-sections of low-voltage power cables

The considered cable is with the cross-section presented in Figure 3-a, with the conductor radius r = 1.8 mm, external sheet radius 12 mm and air gap between conductors. For this cable, parameters appearing in the matrices **Z** and **Y** are: $l_a$=0.565 µH, $l_b$=0.342 µH, $c_a$=86.9 pH, $c_b$=40.2 pH [Grassi].
Simulations are conducted in the frequency range up to 10 MHz. Amplitude characteristic, group delay and input impedance are computed for the couplings when communication equipment is connected between phases *a* and *b* , and *a* and *c* respectively. The third, nonoperating phase is considered to be connected by one of the following ways: via impedance close to the characteristic impedance, open-circuit and short-circuit. High-frequency characteristics computed for the open-circuited and short-circuited nonoperating phase are boundary cases for the termination with an arbitrary impedance. Simulation results for the 50 m long cable are presented in Figures 4, 5 and 6.

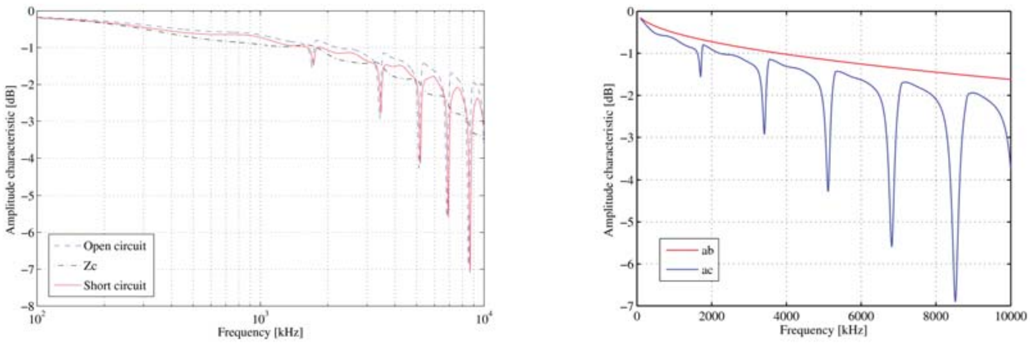


a) Coupling a-c for different nonoperating phase terminations

b) Comparison of couplings a-b and a-c for open non-operating phase

Figure 4. Amplitude characteristics for couplings a-c and a-b in the frequency range up to 10 MHz

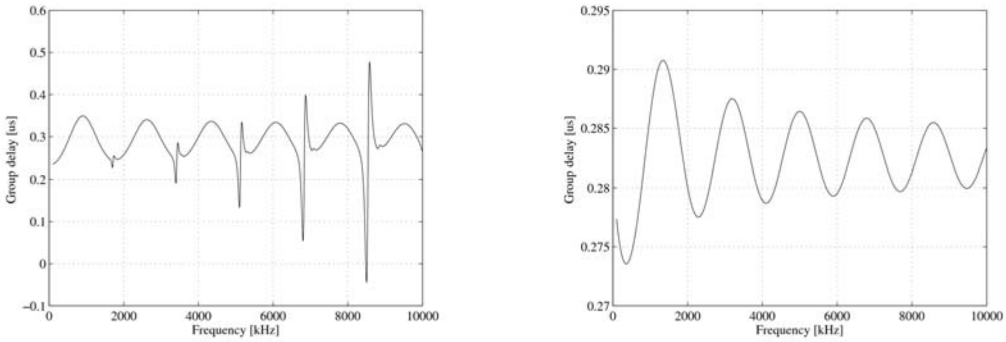


a) Coupling a-c for open nonoperating phase

b) Coupling a-b for open nonoperating phase

Figure 5. Group delay for couplings a-c and a-b in the frequency range up to 10 MHz

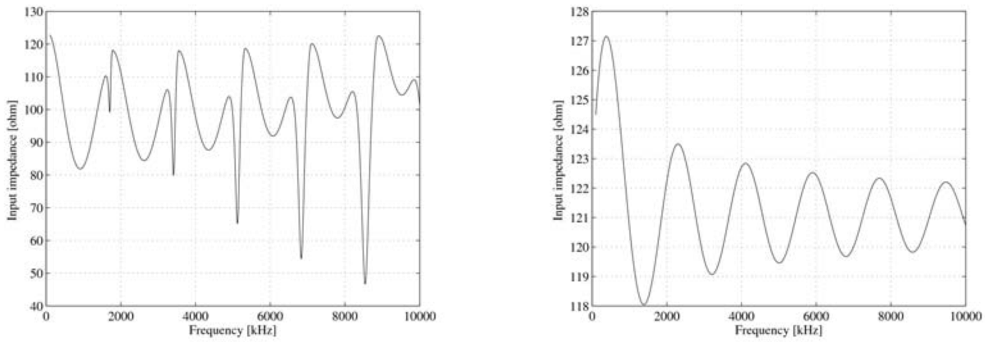


a) Coupling a-c for open nonoperating phase

b) Coupling a-b for open nonoperating phase

Figure 6. Input impedance for couplings a-c and a-b in the frequency range up to 10 MHz

Distribution of the phase voltages among the modal channels, which are independent to each other, is determined by the equation:

$$\mathbf{V}_s = \mathbf{S}^{-1}\mathbf{V} \tag{61}$$

Structure of the matrix $\mathbf{S}^{-1}$ defines three modes, which are graphically described in Figure 7-a, while attenuation of these modes are given in Figure 7-b. It can be observed that coupling between phases *a* and *b* corresponds to the second mode. Therefore, there is no energy exchange between modal channels, what explains that amplitude characteristic and group delay for this coupling are more flat than characteristics of the coupling *a-c*. Oscillations that appear in the coupling *a-b* are forced by the signal reflection only at the line terminals, while coupling *a-c* incorporates interaction between modes.

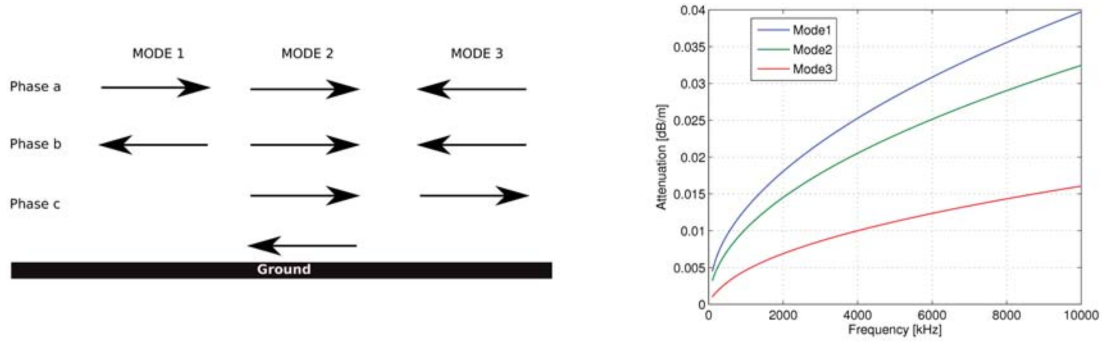


a) Modal channels b) Attenuation of the modal channels

Figure 7. Input impedance for couplings a-c and a-b in the frequency range up to 10 MHz

## 8 Conclusion

This paper presented modelling methodology of communication characteristics of the low-voltage power line. High-frequency characteristics are computed using telegrapher's equations for the multiconductor power line. Telegrapher's equations are solved for the sinusoidal signals, obtaining discrete-frequency communication model. Since communication equipment can be connected to the power line in different manners, denoted as couplings, paper presents algorithm for determination of high-frequency characteristics for different couplings.

Presented methodology is deterministic and based on the knowledge of the power cable impedance and admittance matrices. Branched topology of the power grid can be incorporated in the model by shunt impedances representing frequency-dependent input impedances of the branches.

Simulations are conducted for the 50 m long LV power cable with four round conductors and air-gap between conductors. Results are given in the frequency range up to 10 MHz.

## 9 References

[1] Kostenko, M.V.: *Electromagnetic waves propagation along multiconductor lines*, In: Electrichestvo, No.11, Moscow, 1960, pp. 8- 12. (in Russian)

[2] Sartenaer, T and Delogne, P.: *Deterministic Modeling of the (Shielded) Outdoor Power Line Channel Based on the Multiconductor Transmission Line Equations*, In: IEEE Journal on selected areas in communications, VOL. 24, NO. 7, JULY 2006 , pp. 1277-1291.

[3] Ishkin, V.H. and Shkarin, J.P.: *Computation of parameters of high-frequency channels over overhead power lines*, Technical university of Moscow, Moscow, 1999. (in Russian)

[4] Mikutski,G.V. and Skitalcev, V.S.: *High-frequency links over power lines*, Energoatomizdat, Moscow, 1987. (in Russian)

[5] Wedepohl, L.M.: *Application of matrix methods to the solution of travelling-wave phenomena in polyphase systems*, In: PROC. IEE; 110 (12) (1963) pp. 2200-2212.

[6] Grassi, F.; Pignari, S.A.: *Data-Transmission Characteristics of Power Cables with Star-Quad Cross-Section*, In: IEEE International Symposium on Power Line Communications and Its Applications, 2007. ISPLC '07., 26-28 March 2007 p.p. 401 – 406.